Research Article | Vol. 26, No. 10 | 14 May 2018 | OPTICS EXPRESS 12387

Optics EXPRESS

Optical switching in hybrid VO_2/Si waveguides thermally triggered by lateral microheaters

IRENE OLIVARES,[1] LUIS SÁNCHEZ,[1] JORGE PARRA,[1] ROBERTO LARREA,[1] AMADEU GRIOL,[1] MARIELA MENGHINI,[2] PÍA HOMM,[2] LEE-WOON JANG,[3] BART VAN BILZEN,[2] JIN WON SEO,[3] JEAN-PIERRE LOCQUET,[2] AND PABLO SANCHIS[1,*]

[1]*Nanophotonics Technology Center, Universitat Politècnica de València, Camino de Vera s/n, 46022 Valencia, Spain*
[2]*Department of Physics and Astronomy, KU Leuven, Celestijnenlaan 200D, Leuven, Belgium*
[3]*Department of Materials Engineering, KU Leuven, Kasteelpark Arenberg 44, Leuven, Belgium*
**pabsanki@ntc.upv.es*

Abstract: The performance of optical devices relying in vanadium dioxide (VO_2) technology compatible with the silicon platform depends on the polarization of light and VO_2 properties. In this work, optical switching in hybrid VO_2/Si waveguides thermally triggered by lateral microheaters is achieved with insertion losses below 1 dB and extinction ratios above 20 dB in a broad bandwidth larger than 30 nm. The optical switching response has been optimized for TE and TM polarizations by using a homogeneous and a granular VO_2 layer, respectively, with a small impact on the electrical power consumption. The stability and reversibility between switching states showing the possibility of bistable performance is also demonstrated.

OCIS codes: (130.4815) Optical switching devices; (230.7370) Waveguides; (250.5300) Photonic integrated circuits.

References and links

1. V. J. Sorger, N. D. Lanzillotti-Kimura, R. M. Ma, and X. Zhang, "Ultra-compact silicon nanophotonic modulator with broadband response," Nanophotonics **1**(1), 17–22 (2012).
2. H. Zhang, L. Zhou, B. M. A. Rahman, X. Wu, L. Lu, Y. Xu, J. Xu, J. Song, Z. Hu, L. Xu, and J. Chen, "Ultracompact Si-GST Hybrid Waveguides for Nonvolatile Light Wave Manipulation," IEEE Photonics J. **10**(1), 1–10 (2018).
3. H. Liang, R. Soref, J. Mu, A. Majumdar, X. Li, and W. P. Huang, "Simulations of Silicon-on-Insulator Channel-Waveguide Electrooptical 2× 2 Switches and 1× 1 Modulators Using a $Ge_2Sb_2Te_5$ Self-Holding Layer," J. Lightwave Technol. **33**(9), 1805–1813 (2015).
4. G. Seo, B. J. Kim, C. Ko, Y. Cui, Y. W. Lee, J. H. Shin, S. Ramanathan, and H. T. Kim, "Voltage-pulse induced switching dynamics in VO_2 thin films devices on silicon," IEEE Electron. Dev. Lett. **32**(11), 1582–1584 (2011).
5. Z. Yang, C. Ko, and S. Ramanathan, "Oxide electronics utilizing ultrafast metal-insulator transitions," Annu. Rev. Mater. Res. **41**(1), 337–367 (2011).
6. W. A. Vitale, E. A. Casu, A. Biswas, T. Rosca, C. Alper, A. Krammer, G. V. Luong, Q. T. Zhao, S. Mantl, A. Schüler, and A. M. Ionescu, "A steep-slope transistor combining phase-change and band-to-band-tunneling to achieve a sub-unity body factor," Sci. Rep. **7**(1), 355–365 (2017).
7. C. Ko, and S. Ramanathan, "Observation of electric field assisted phase transition in thin film vanadium oxide in a metal oxide semiconductor device geometry," Appl. Phys. Lett. **93**(25), 1–4 (2008).
8. A. Zimmers, L. Aigouy, M. Mortier, A. Sharoni, S. Wang, K. G. West, J. G. Ramirez, and I. K. Schuller, "Role of thermal heating on the voltage induced insulator-metal transition in VO_2," Phys. Rev. Lett. **110**(5), 056601 (2013).
9. M. A. Kats, R. Blanchard, P. Genevet, Z. Yang, M. M. Qazilbash, D. N. Basov, S. Ramanathan, and F. Capasso, "Thermal tuning of mid-infrared plasmonic antenna arrays using a phase change material," Opt. Lett. **38**(3), 368–370 (2013).
10. B. G. Chae, H. T. Kim, D. H. Youn, and K. Y. Kang, "Abrupt metal–insulator transition observed in VO_2 thin films induced by a switching voltage pulse," Phys. B Condens. Matter **369**(1–4), 76–80 (2005).
11. D. Ruzmetov, G. Gopalakrishnan, J. Deng, V. Narayanamurti, and S. Ramanathan, "Electrical triggering of metal-insulator transition in nanoscale vanadium oxide junctions," J. Appl. Phys. **106**(8), 1–6 (2009).
12. S. B. Lee, K. Kim, J. S. Oh, B. Kahng, and J. S. Lee, "Origin of variation in switching voltages in threshold-switching phenomena of VO_2 thin films," Appl. Phys. Lett. **102**(6), 1–6 (2013).

#326541 https://doi.org/10.1364/OE.26.012387
Journal © 2018 Received 21 Mar 2018; revised 25 Apr 2018; accepted 26 Apr 2018; published 30 Apr 2018

Optics EXPRESS

13. A. Joushaghani, J. Jeong, S. Paradis, D. Alain, J. Stewart Aitchison, and J. K. S. Poon, "Voltage-controlled switching and thermal effects in VO_2 nano-gap junctions," Appl. Phys. Lett. **104**(22), 1–5 (2014).
14. P. Markov, R. E. Marvel, H. J. Conley, K. J. Miller, R. F. Haglund, Jr., and S. M. Weiss, "Optically monitored electrical switching in VO_2," ACS Photonics **2**(8), 1175–1182 (2015).
15. Z. Yang, S. Hart, C. Ko, A. Yacoby, and S. Ramanathan, "Studies on electric triggering of the metal-insulator transition in VO_2 thin films between 77 K and 300 K," J. Appl. Phys. **110**(3), 033725 (2011).
16. J. Yoon, G. Lee, C. Park, B. S. Mun, and H. Ju, "Investigation of length-dependent characteristics of the voltage-induced metal insulator transition in VO_2 film devices," Appl. Phys. Lett. **105**(8), 083503 (2014).
17. L. Sánchez, A. Rosa, A. Griol, A. Gutierrez, P. Homm, B. Van Bilzen, M. Menghini, J. P. Locquet, and P. Sanchis, "Impact of the external resistance on the switching power consumption in VO_2 nano gap junctions," Appl. Phys. Lett. **111**(3), 031904 (2017).
18. J. D. Ryckman, V. Diez-Blanco, J. Nag, R. E. Marvel, B. K. Choi, R. F. Haglund, and S. M. Weiss, "Photothermal optical modulation of ultra-compact hybrid Si-VO_2 ring resonators," Opt. Express **20**(12), 13215–13225 (2012).
19. J. D. Ryckman, K. A. Hallman, R. E. Marvel, R. F. Haglund, and S. M. Weiss, "Ultra-compact silicon photonic devices reconfigured by an optically induced semiconductor-to-metal transition," Opt. Express **21**(9), 10753–10763 (2013).
20. E. Abreu, S. N. Gilbert Corder, S. Jin Yun, S. Wang, J. G. Ramírez, K. West, J. Zhang, S. Kittiwatanakul, I. K. Schuller, J. Lu, S. A. Wolf, H.-T. Kim, M. Liu, and R. D. Averitt, "Ultrafast electron-lattice coupling dynamics in VO2 and V_2O_3 thin films," Phys. Rev. B **96**(9), 094309 (2017).
21. L. Sánchez, S. Lechago, and P. Sanchis, "Ultra-compact TE and TM pass polarizers based on vanadium dioxide on silicon," Opt. Lett. **40**(7), 1452–1455 (2015).
22. A. Joushaghani, J. Jeong, S. Paradis, D. Alain, J. Stewart Aitchison, and J. K. S. Poon, "Wavelength-size hybrid Si-VO_2 waveguide electroabsorption optical switches and photodetectors," Opt. Express **23**(3), 3657–3668 (2015).
23. L. Sánchez, F. C. Juan, A. Rosa, and P. Sanchis, "Ultra-compact electro-absorption VO_2–Si modulator with TM to TE conversion," J. Opt. **19**(3), 035401 (2017).
24. L. Sanchez, S. Lechago, A. Gutierrez, and P. Sanchis, "Analysis and Design Optimization of a Hybrid VO_2/Silicon 2x2 Microring Switch," IEEE Photonics J. **8**(2), 1–9 (2016).
25. M. Sun, W. Shieh, and R. R. Unnithan, "Design of Plasmonic Modulators with Vanadium Dioxide on Silicon-on-Insulator," IEEE Photonics J. **9**(3), 1–10 (2017).
26. K. J. Miller, K. A. Hallman, R. F. Haglund, and S. M. Weiss, "Silicon waveguide optical switch with embedded phase change material," Opt. Express **25**(22), 26527–26536 (2017).
27. J. K. Clark, Y. L. Ho, H. Matsui, and J. J. Delaunay, "Optically Pumped Hybrid Plasmonic-Photonic Waveguide Modulator Using the VO_2 Metal-Insulator Phase Transition," IEEE Photonics J. **10**(1), 1–9 (2018).
28. S. Kumar, M. D. Pickett, J. P. Strachan, G. Gibson, Y. Nishi, and R. S. Williams, "Local Temperature Redistribution and Structural Transition During Joule-Heating-Driven Conductance Switching in VO_2," Adv. Mater. **25**(42), 6128–6132 (2013).
29. B. S. Mun, J. Yoon, K. S. Mo, K. Chen, N. Tamura, C. Dejoie, M. Kunz, Z. Liu, C. Park, K. Moon, and H. Ju, "Role of joule heating effect and bulk-surface phases in voltage-driven metal-insulator transition in VO_2 crystal," Appl. Phys. Lett. **103**(6), 061902 (2013).
30. E. Freeman, G. Stone, N. Shukla, H. Paik, J. A. Moyer, Z. Cai, H. Wen, R. E. Herbert, D. G. Schlom, V. Gopalan, and S. Datta, "Nanoscale structural evolution of electrically driven insulator to metal transition in vanadium dioxide," Appl. Phys. Lett. **103**(26), 263109 (2013).
31. G. Gopalakrishnan, D. Ruzmetov, and S. Ramanathan, "On the triggering mechanism for the metal–insulator transition in thin film VO_2 devices: electric field versus thermal effects," J. Mater. Sci. **44**(19), 5345–5353 (2009).
32. J. Leroy, A. Crunteanu, A. Bessaudou, F. Cosset, C. Champeaux, and J. C. Orlianges, "High-speed metal-insulator transition in vanadium dioxide films induced by an electrical pulsed voltage over nano-gap electrode," Appl. Phys. Lett. **100**(21), 213507 (2012).
33. X. Xu, X. He, H. Wang, Q. Gu, S. Shi, H. Xing, Ch. Wang, J. Zhang, X. Chen, and J. Chu, "The extremely narrow hysteresis width of phase transition in nanocrystalline VO_2 thin films with the flake grain structures," Appl. Surf. Sci. **261**, 83–87 (2012).
34. S. Kumar, D. Lenoble, F. Maury, and N. Bahlawane, "Synthesis of vanadium oxide films with controlled morphologies: Impact on the metal–insulator transition behavior," Phys. Status Solidi **212**(7), 1582–1587 (2015).
35. G. Guzman, R. Morineau, and J. Livage, "Synthesis of vanadium dioxide thin films from vanadium alkoxides," Mater. Res. Bull. **29**(5), 509–515 (1994).
36. W. Gao, C. M. Wang, H. Q. Wang, V. E. Henrich, and E. I. Altman, "Growth and surface structure of vanadium oxide on anatase," Surf. Sci. **559**(2–3), 201–213 (2004).
37. A. P. Peter, K. Martens, G. Rampelberg, M. Toeller, J. M. Ablett, J. Meersschaut, D. Cuypers, A. Franquet, C. Detavernier, J. P. Rueff, M. Schaekers, S. Van Elshocht, M. Jurczak, Ch. Adelmann, and I. P. Radu, "Metal Insulator Transition in ALD VO_2 Ultrathin Films and Nanoparticles: Morphological Control," Adv. Funct. Mater. **25**(5), 679–686 (2015).

Optics EXPRESS

38. Á. Rosa, A. Gutiérrez, A. Brimont, A. Griol, and P. Sanchis, "High performace silicon 2x2 optical switch based on a thermo-optically tunable multimode interference coupler and efficient electrodes," Opt. Express **24**(1), 191–198 (2016).
39. B. Van Bilzen, P. Homm, L. Dillemans, C.-Y. Su, M. Menghini, M. Sousa, C. Marchiori, L. Zhang, J. W. Seo, and J.-P. Locquet, "Production of VO_2 thin films through post-deposition annealing of V_2O_3 and VO_x films," Thin Solid Films **591**, 143–148 (2015).

1. Introduction

The silicon photonics platform combined with disruptive materials will provide hybrid technologies able to overcome the challenging requirements in current photonic systems [1–3]. Several phase transition materials have been proposed as active materials to enhance the performance of optical devices based on silicon photonics. Among them, vanadium dioxide (VO_2) has reached an outstanding performance due to its reversible and sharp insulator-metal transition (IMT) near room temperature [4–6]. Remarkable changes in electrical and optical properties of the active material can be obtained when controlling the phase transition by means of external stimuli like temperature [7–9], electric field [10–17] or optical pumping [18-20]. The change in the optical properties of the material is useful for the design of ultra-compact optical devices based on the hybrid VO_2/Si technology [21–27]. Nevertheless, the phase transition in VO_2 is still the subject of intense discussion. Several works in the literature have studied the IMT in VO_2 induced by applying an external electric field to elucidate whether the mechanism of the transition is related to solely a Joule-heating process [8, 28, 29], to the electric field contribution [15, 30–32] or a combination of both effects. Furthermore, the structural properties of the VO_2 layer seem to have a key role on the phase transition. It has been shown that crystalline quality, sample morphology and surface roughness are important characteristics influencing the hysteresis cycle [33, 34]. Polycrystalline and epitaxial layers have been grown using different deposition techniques [34–37], however, controlling process conditions is key to obtain good film quality.

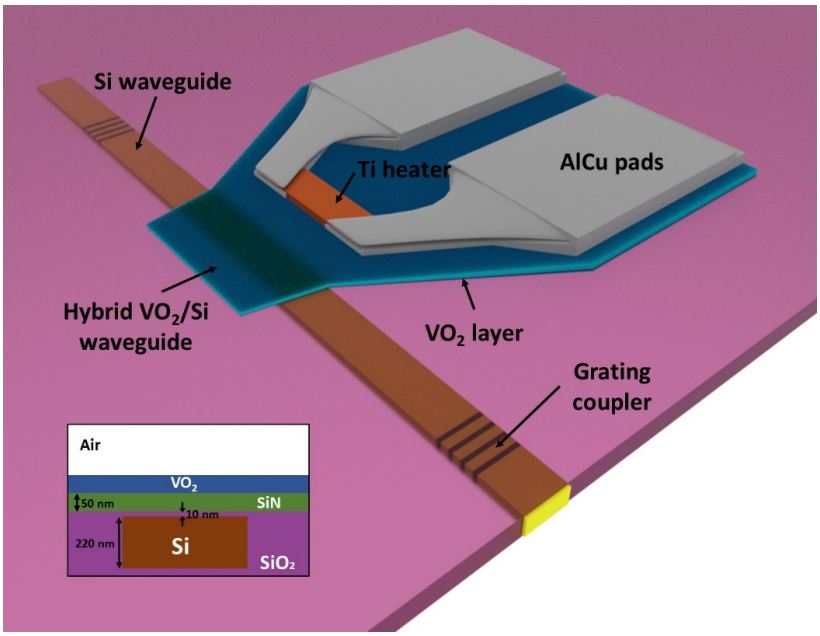

Fig. 1. Concept art of the hybrid VO_2/Si waveguide with a lateral Ti microheater based on a double metallization process. The inset shows the cross section of the hybrid VO_2/Si waveguide. The silicon waveguide has a width of 480 nm and a thickness of 220 nm. The inset shows the spacer between the silicon waveguide and the VO_2 layer that is made of a 10 nm-thick oxide layer plus a 50 nm-thick nitride (SiN) hardmask. The SiN layer is needed for planarization and protection of the silicon surface.

Optics EXPRESS

In this work, optical switching is demonstrated in a hybrid VO_2/Si waveguide by means of lateral resistive microheaters as shown in Fig. 1. The microheaters are based on a double metallization process to efficiently focus the generated heat on the hybrid waveguide [38]. Thus, the VO_2 layer on top of the silicon waveguide is switched from the insulating to the metallic state, changing significantly the optical losses in a very short length. Furthermore, the effect of the morphology of the VO_2 layers on the optical switching performance has also been experimentally analyzed and demonstrated to achieve a similar behavior for both light polarizations independently of the structural properties of the VO_2 layer. An electrical power consumption for a complete VO_2 phase transition ranging between 30 mW and 85 mW has been achieved, which is more than one order of magnitude lower compared to previous works based also on a Joule heating approach [26]. Lower power consumptions have been reported by triggering the VO_2 phase transition by a carrier injection approach but at expenses of higher insertion losses and lower extinction ratios [14, 22].

2. Description of the hybrid VO_2/Si waveguide

A concept art of the hybrid VO_2/Si waveguide with a lateral microheater is shown in Fig. 1. The silicon waveguide has a cross section of 480 nm x 220 nm. A VO_2 patch with a length of 20 µm is deposited to form the hybrid waveguide. The spacer between the silicon waveguide and the VO_2 layer is made of a 10 nm-thick oxide layer plus a 50 nm-thick nitride (SiN) hardmask. The SiN layer is needed for planarization and protection of the silicon surface. The VO_2 layer is also extended below the heater as depicted in Fig. 1. The heater is based on a double metallization process with a lateral displacement of 550 nm to avoid optical losses due to the proximity of the metals to the hybrid waveguide. A voltage is applied on the low resistance AlCu pads, so that the current is mainly determined by the Ti section, which short-circuits the pads. Therefore, the heat is efficiently transferred to the VO_2 patch placed over the waveguide, minimizing the electrical power consumption.

The optical losses of the hybrid VO_2/Si waveguide depend on the state of the VO_2. At steady conditions, the VO_2 is in the insulating state and the material introduces a low level of optical losses. When an electrical power is applied to the heater, a temperature gradient determines the VO_2 areas that will switch to the metallic state. By applying sufficient electrical power, the generated heat is high enough to induce the phase transition in the whole VO_2 placed over the waveguide [26, 28]. Therefore, the optical losses are drastically increased and an optical switching with high extinction ratio is achieved.

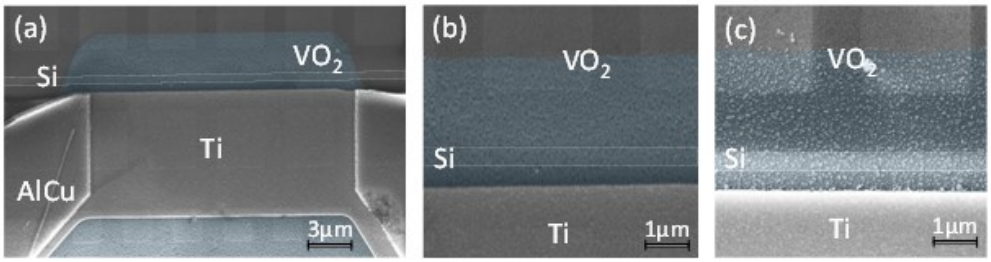

Fig. 2. (a) SEM image of the hybrid VO_2/Si waveguide with a lateral microheater. The silicon waveguide contour has been outlined and the VO_2 region has been highlighted with a false color for clarity. Zoom over the hybrid VO_2/Si area of two different waveguides with (b) homogenous and (c) granular VO_2 layer.

The described hybrid VO_2/Si waveguides have been fabricated on a SOI wafer with a buried oxide layer thickness of 2 µm. The silicon waveguide structures were first fabricated by a standard process. The wafer was then polished by chemical mechanical planarization (CMP) and diced for VO_2 deposition and electrodes patterning. A 40-nm thick amorphous VO_x layer has been grown by molecular beam epitaxy (MBE). After the deposition, a lift-off

Optics EXPRESS

process was done to remove the VO_x deposited on the undesired regions. Finally, an ex-situ annealing process is carried out to form a polycrystalline VO_2 layer [39]. The electrodes have been fabricated by two e-beam positive resist exposure prior to metal evaporation and lift-off processes [38]. First, a 90 nm-thick Ti was processed and then 400 nm-thick AlCu pads were deposited.

Figure 2(a) shows a SEM image of the fabricated hybrid VO_2/Si waveguide with the lateral microheater. Identical structures albeit with different grating couplers were fabricated to test the optical switching performance for both TE and TM polarizations. By changing the processing conditions, the morphology of the VO_2 film could be modified such that a granular VO_2 layer, instead of a homogeneous one, was obtained. The granular morphology was the result of an additional solvent bath step during the exposure/lift-off processes. Furthermore, the thickness and roughness of the VO_2 layer was also measured by Atomic Force Microscopy (AFM) after the electrodes fabrication. A thickness of around 15 nm with a roughness of 10 nm was obtained in the sample with granulated VO_2 compared to a thickness of 30 nm with a roughness of 6 nm obtained in the sample with homogeneous VO_2. Figure 2(b) shows a zoom-in on the hybrid VO_2/Si waveguide with a homogenous VO_2 layer while Fig. 2(c) depicts the hybrid waveguide with a granular VO_2 layer.

3. Experimental results

3.1 Insulator-metal transition of the VO_2 active material

The electrical resistivity was first characterized as a function of temperature in VO_2 test patches deposited on the same wafers having the hybrid VO_2/Si waveguides after ex-situ annealing. The results obtained for the homogenous and granular VO_2 are shown in Fig. 3. The insulator to metal phase transition is clearly observed for both cases. The transition occurs at around 75°C for the heating up process while the reversed transition (metal to insulator) occurs at 65°C along the cooling down process, which implies a hysteresis width of 10°C and a transition temperature of 70°C. The single-phase character of the VO_2 layer is confirmed by the transition temperature being close to the reported value for bulk samples. However, a higher overall resistivity and a slightly lower resistivity change across the phase transition is achieved in the granular VO_2.

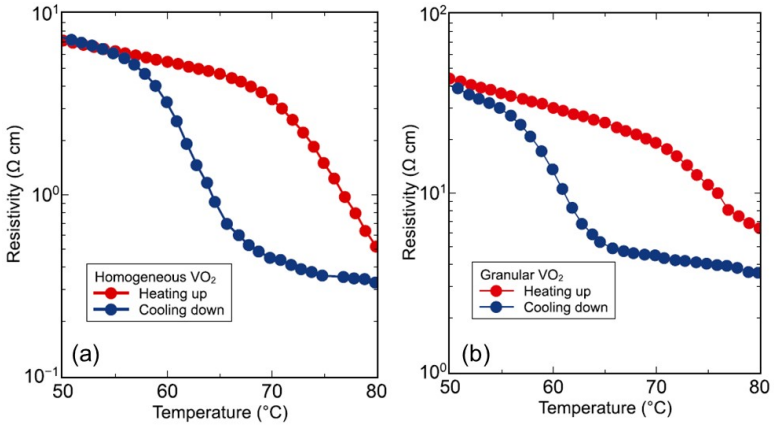

Fig. 3. Electrical resistivity of the (a) homogenous and (b) granular VO_2 layers as a function of temperature after ex-situ annealing. The one order of magnitude change in resistivity as the temperature increases, indicating an IMT at 70°C, confirms the transformation to VO_2 in both samples.

Optics EXPRESS

3.2 Optical switching performance of the hybrid VO_2/Si waveguides

The optical switching performance of the hybrid VO_2/Si waveguides has been characterized by applying a voltage to the electrodes and measuring the variation of the optical power at the output. In addition, the applied electrical power was obtained by simultaneously measuring the electrical current flowing through the electrodes. The light from a continuous-wave (CW) laser was injected into the chip and extracted at the output through the grating couplers. The polarization of the injected light was adjusted with an external polarization controller. The output light was photodetected and measured with a power meter. The electro-optical responses for the different types of VO_2 morphologies are shown in Fig. 4 for TE polarization and in Fig. 5 for TM polarization. For both polarizations, it can be clearly seen that the variation of the optical power has a hysteretic response in agreement with the change of the electrical resistivity with temperature observed in Fig. 3, which confirms the existence of the phase transition regardless the morphology of the VO_2 film. The transition from the insulating to the metallic state is achieved by heating the VO_2 (heating up process) while the VO_2 is switched back from the metallic to the insulating state by decreasing the electrical power and therefore decreasing the heat applied to the hybrid waveguide (cooling down process).

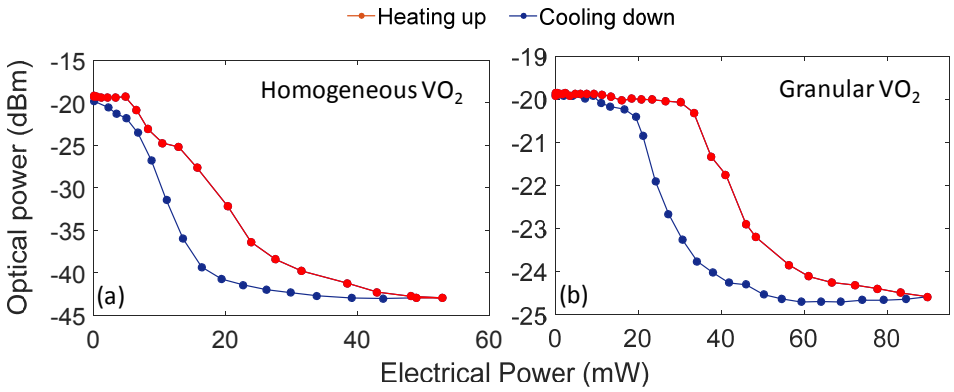

Fig. 4. Variation of optical power as a function of the applied electrical power for TE polarization in the hybrid VO_2/Si waveguide with (a) homogeneous and (b) granular VO_2.

Nevertheless, marked switching differences can be appreciated depending on the VO_2 morphology and the polarization of the light. For TE polarization, the optical losses at steady conditions, i.e. without applying any electrical power, are similar for both hybrid VO_2/Si waveguides with homogenous [Fig. 4(a)] and granular [Fig. 4(b)] VO_2 layers. However, a much larger variation of the optical power when switching towards the metallic state (>20 dB) and a smaller power consumption is achieved for the case of the structure with the homogenous VO_2 layer, which makes this waveguide configuration preferable for TE polarization. The smaller power consumption is attributed to a more efficient heat transfer through the homogenous VO_2 film from the heater to the top of the optical waveguide and therefore independent of the light polarization.

Optics EXPRESS

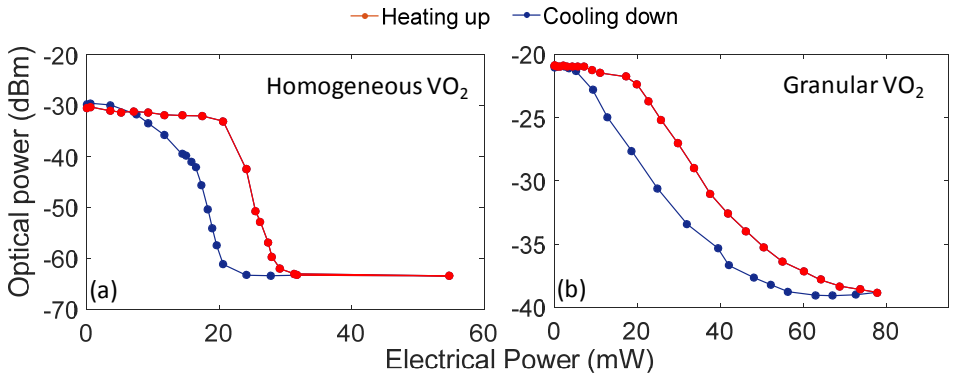

Fig. 5. Variation of optical power as a function of the applied electrical power for TM polarization in the hybrid VO_2/Si waveguide with (a) homogeneous and (b) granular VO_2.

The optimum switching structure for TM polarization is the opposite compared to TE polarization. In this case, optical losses at steady conditions are almost 10 dB higher for the hybrid waveguide with the homogenous VO_2 layer, Fig. 5(a). Therefore, the waveguide with the granular VO_2 layer is more attractive despite the larger power consumption. Furthermore, as there is a stronger interaction of light with the VO_2 layer compared to TE polarization, a variation of optical losses above 20 dB is still achieved as it can be seen in Fig. 5(b).

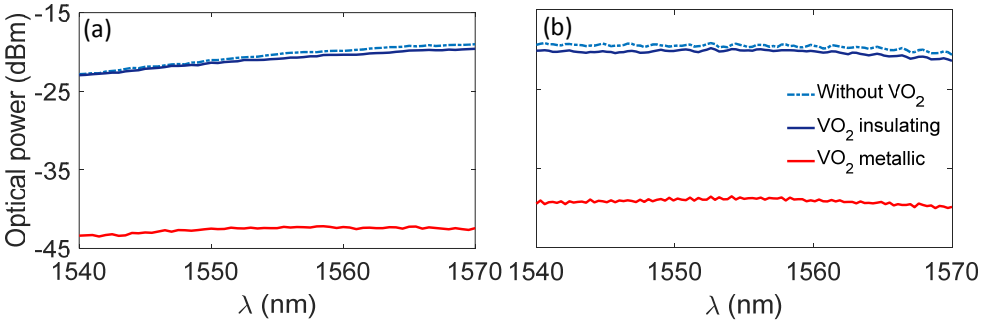

Fig. 6. Transmission spectra of a Si waveguide and the hybrid VO_2/Si waveguide (a) with homogeneous VO_2 layer and TE polarization and (b) with the granular VO_2 and TM polarization. The VO_2 metallic state is achieved by applying an electrical power of around (a) 45 mW for TE and (b) 70 mW for TM.

The transmission spectrum of the hybrid VO_2/Si waveguide is shown for TE polarization and homogeneous VO_2 in Fig. 6(a) and for TM polarization and the granular VO_2 in Fig. 6(b). A similar response is obtained for both polarizations showing that changing the VO_2 morphology could be an easy and cost-effective approach to achieve hybrid VO_2/Si structures with optimized performance for the target polarization. Insertion losses are almost negligible as it can be observed in Fig. 6 when comparing the response of the hybrid waveguide with VO_2 in the insulating state with the response of a silicon waveguide without VO_2 fabricated on the same sample. It should be noticed that the effective thickness of the VO_2 layer is smaller in the hybrid waveguide with granulated VO_2, which also contributes to reduce insertion losses. An extinction ratio higher than 20 dB is achieved for both polarizations when the VO_2 is switched to the metallic state with a power consumption of ~45 mW for TE and of ~70 mW for TM. Furthermore, the optical switching bandwidth is maintained very broad (>30 nm) regardless of the morphology of the VO_2. The wavelength range shown in Fig. 6 was determined by the bandwidth of the CW laser used in the measurements.

Optics EXPRESS

3.3 Temporal switching performance and bistability

The optical switching performance of the hybrid VO_2/Si waveguide can be stabilized at any point of the hysteresis cycle just by changing the applied electrical power and, hence, film temperature. The performance of the hybrid waveguide with granular VO_2 has been used to analyze if the morphology of the VO_2 could have an influence on the temporal response. Measurements have been carried out by supplying electrical voltage pulses with a duration of several seconds on the electrodes. Figure 7(a) shows the switching operation for TM polarization between minimum and maximum optical levels of the hysteresis cycle exploiting the full VO_2 phase transition. In this case, the smallest insertion losses and maximum extinction ratio are achieved. Figure 7(b) shows the temporal response of the electrical power (EP) applied to the electrodes and the corresponding normalized optical power (NOP). The switching between states is clearly stable and reversible.

On the other hand, different working points along the hysteresis curve can be chosen to take advantage of the VO_2 bistability feature. An example is shown in Fig. 7(c) with the selected points marked in grey. Two different states in terms of optical losses, state 1 and state 2, can be achieved by using the same electrical signal applied to the electrodes (~25 mW). A short voltage pulse is applied to change between both states. The temporal response in terms of EP and NOP is depicted in Fig. 7(d). For switching from state 1 to state 2, the electrical power must be increased to complete the insulator to metal transition. This is achieved by applying a positive electric pulse and therefore increasing the power applied to the electrodes. On the other hand, the switching from state 2 to state 1 is achieved by applying a negative electric pulse such that the electrical power applied to the electrode is zero during the time of the pulse. The fastest switching speed was measured in the microsecond range consistent with a thermal based operation. Furthermore, the same temporal switching performance was also measured for the hybrid waveguide with homogeneous VO_2.

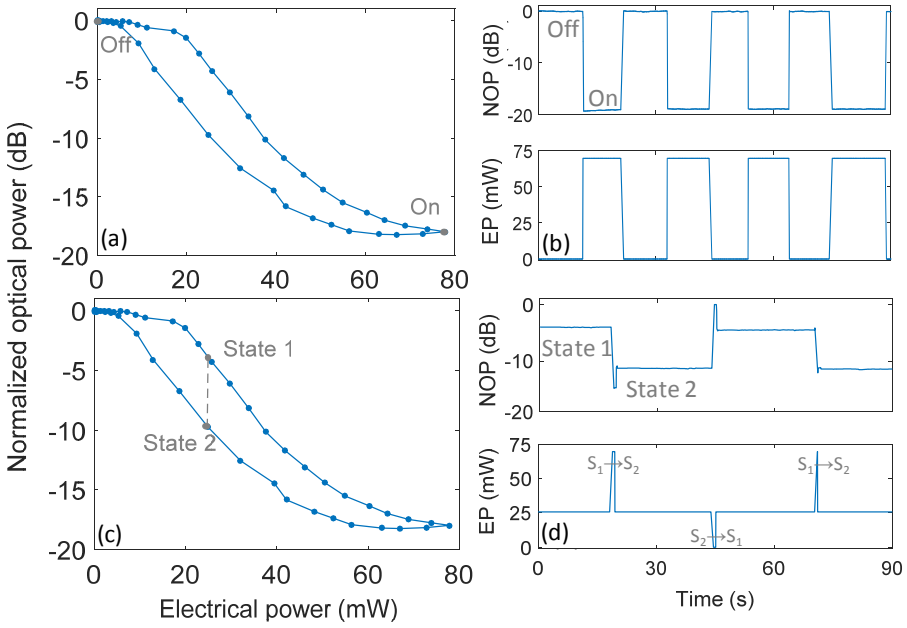

Fig. 7. (a) Scheme of the switching process between maximum (Off) and minimum (On) optical levels and (b) electrical power (EP) of applied voltage pulses as a function of time and the corresponding response of the normalized optical power (NOP). (c) Scheme of the bistable switching performance between State 1 and State 2 and (d) temporal responses of EP and the corresponding NOP for successive reversible switching between both states.

Optics EXPRESS

4. Conclusions

Thermally triggered optical switching in hybrid VO_2/Si waveguides has been proposed and demonstrated by using a lateral microheater based on a double metallization process. Furthermore, the impact of the VO_2 layer morphology on the switching performance has been analyzed and exploited to have the best features depending on the light polarization. Therefore, insertion losses below 1 dB and extinction ratios above 20 dB have been achieved with an active length of only 20 μm and an electrical power consumption of around 45 mW for TE polarization and 70 mW for TM polarization. The electro-optical switching response has a broadband performance above 30 nm and is temporally stable and reversible. Furthermore, a bistable switching performance has also been shown by exploiting the hysteretic response of the VO_2 phase transition. Such feature could be useful for implementing optical based memristors or microscale memories with optical readout functionality.

Funding

Funding from project TEC2016-76849 (MINECO/FEDER, UE) and H2020-PHRESCO (688579) is acknowledged. The SOI samples were fabricated at IHP (we acknowledge Lars Zimmermann) in the framework of FP7-ICT-2013-11-619456 SITOGA project. Irene Olivares and Roberto Larrea also acknowledge respectively the Universitat Politècnica de València and the Ecuadorian Government for funding their grant. P.H. acknowledges support from Becas Chile-CONICYT.